Radiation Effects, 1981, Vol. 55, pp. 209–222
0033-7579/81/5504–0209$06.50/0

AN ANALYTICAL APPROACH TO VOID GROWTH IN METALS UNDER INTENSE RADIATION PULSING

N. M. GHONIEM

School of Engineering and Applied Science University of California-Los Angeles, Los Angeles, CA. 90024, U.S.A.

and

H. GUROL

Department of Chemical and Nuclear Engineering, University of California-Santa Barbara, Santa Barbara, CA., U.S.A.

(*Received July 16, 1980; in final form January 22, 1981*)

Reprinted from *Radiation Effects*, Volume 55, Nos. 3 and 4

23

9N

Radiation Effects, 1981, Vol. 55, pp. 209–222
0033-7579/81/5504–0209$06.50/0

AN ANALYTICAL APPROACH TO VOID GROWTH IN METALS UNDER INTENSE RADIATION PULSING

N. M. GHONIEM

School of Engineering and Applied Science University of California-Los Angeles, Los Angeles, CA. 90024, U.S.A.

and

H. GUROL

Department of Chemical and Nuclear Engineering, University of California-Santa Barbara, Santa Barbara, CA., U.S.A.

(Received July 16, 1980; in final form January 22, 1981)

1 INTRODUCTION

Many of the proposed fusion reactor concepts[1–3] are designed to operate in a cyclic mode. During the burn cycle, thermonuclear energy is primarily delivered to the reactor first wall and blanket; and during the cool cycle, the initial reactor conditions are re-established. In the case of Inential Confinement Fusion Reactors (ICFR's), the production of thermonuclear energy and the ensuing radiation damage to reactor components occur in a very short period of time (less than a microsecond[4]). This is followed by a relatively long down time (on the order of a fraction of a second). The extremely small duty factors in ICFR's (on-time/cycle time) pose some interesting problems related to the behavior of the damage-produced defects.

The interest in experimental and theoretical methods for pulsed damage analysis has been increasing in the last few years. The small number of pulsed irradiation experiments performed to date[5–11] have demonstrated the significant differences in the response of materials to pulsed irradiation when compared to steady irradiation. On the theoretical side, various models have been recently used to analyze aspects of microstructural behavior during irradiation. Rate theory models have been applied to point defect behavior,[12] void nucleation,[13,14] void growth and swelling,[15–19] defect buildup and solute segregation,[20] irradiation creep[21,22] and finally void and loop nucleation and growth.[23]

In most of the theoretical models, the numerical integration of a large system of non-linear, coupled differential equations places severe computational limitations, especially when the solution is required after many pulses. Aside from numerical error control problems that can arise when the stiff system of differential equations is integrated with a pulsed source term, the solution can be unrealistically expensive for the millions of pulses expected over the wall lifetime in an ICFR. Furthermore, fusion reactor concepts, particularly for inertial confinement fusion, are still evolving and continuously changing. A model that is physically based and computationally simple can be very useful in reactor design sensitivity studies.

In a previous paper, a Fully Dynamic Rate Theory (FDRT) was developed[16] for studying the void swelling of metals irradiated with time-varying irradiation sources. This theory was then further utilized in a numerical integration scheme[17] in order to evaluate the void swelling of pulsed fusion reactors. In the present paper, we present an analytical method to study void growth in ICFR first walls. The analytical approach is intended to be used for the description of the long term behavior of irradiation-induced voids in ICFR's. A large combination of material and irradiation variables can thus be studied in preliminary investigations of reactor parameters.

2 ANALYTICAL MODEL

The solution of the diffusion equation for point defects in the vicinity of a spherical cavity of radius R yields the following void growth equation

$$\frac{dR}{dt} = \frac{1}{R}\left\{D_v C_v - D_i C_i - D_v C_v^e\left(\exp\left(\frac{2\gamma\Omega}{Rk_B T_i}\right) - 1\right)\right\}. \quad (1)$$

The symbols and parameters used in Eq. (1) and all following equations are listed in the nomenclature at the end of this paper.

Before attempting to solve Eq. (1), the explicit time dependence of point defect concentrations $C_{v,i}$ has to be specified. In our analysis, we will use Eq. (1) to describe void behavior during steady-state irradiation, and then proceed to a comparison of this behavior during the equivalent pulsed irradiation.

2.1 *Model Assumptions and Limitations*

Since the basic motivation behind the development of the present analytical model is to describe void behavior in ICFR first walls without excessive computations, the model will rely on certain simplifying assumptions. This will in turn limit the applicability of the model to cases where the assumptions are valid.

Point defects are assumed here to diffuse in a uniform, homogeneous medium. Vacancy loops resulting from collision cascades are considered a part of the overall sink, which is expressed as a constant dislocation density, ρ_d cm/cm^3. After immediate point defect recombination in cascades, a net production rate of P at/at/second is established in the bulk material of the first wall. This also implies that cascade overlap effects should be considered in the final evaluation of the point defect production rate. The diffusion of vacancies to sinks is described by a mean lifetime, τ_v, while that for interstitials is described by τ_i. This lifetime description is obviously valid only after the initial damage production state, and is therefore regarded accurate for point defect diffusion to pre-existing voids. The present study will focus on the inter-pulse behavior of a preconditioned microstructure (i.e., in the growth or shrinkage phase).

Modeling of the interstitial loop microstructure evolution is implicitly included in a constant initial dislocation density. The only microstructural feature that is allowed to change with irradiation is the void microstructure. In principle, interstitial loops can also be included in the present analytical model. However, the fact that this analysis applies past the void nucleation time immediately implies the presence of a more or less stable dislocation density.[24]

It is also assumed in our analysis that the cavities are formed by the condensation of irradiation produced vacancies and do not contain gas atoms from nuclear reactions. The analysis is therefore limited to inertial confinement designs where the He/dpa ratio is low and voids rather than helium filled cavities are expected to dominate. Even though an analytical solution including helium effects would be more complex, it is still possible to incorporate a separate rate equation for helium diffusion and to include a gas pressure term in treating the growth and shrinkage kinetics of cavities.

2.2 *Steady-Irradiation Analysis*

The term steady-irradiation is used here to indicate that the source of irradiation is time-independent. The state of the irradiated material is best described as being in a quasi-steady-state. Changes in point defect lifetimes due to microstructure evolution are usually small as to validate the steady-state assumptions within a prescribed time period.

During steady-state, the concentrations of point defects are determined by the balance between production and destruction rates. A point defect mean lifetime, τ, is defined as the average time spent in the matrix before a point defect is absorbed at the various microstructural components. For vacancies (v) and interstitials (i), the lifetimes can be written as:

$$\tau_{v,i} \simeq \frac{1}{D_{v,i}(Z_{v,i}\rho_d + 4\pi RN)}. \quad (2)$$

Assuming that the dislocation density, ρ_d, does not change with time, we define:

$$\chi(t) = \frac{4\pi R(t)N}{\rho_d} \quad (3)$$

as the ratio of the void sink strength to the dislocation sink strength. Equation (2) can then be written as:

$$\tau_{v,i} \simeq \{Z_{v,i}\rho_d D_{v,i}(1 + \chi(t))\}^{-1}. \quad (4)$$

If we choose a time interval, Δt, such that $\chi(t)$ is approximately constant, we have the quasi-steady

state (QSS) point defect equations

$$\frac{dC_{v,i}}{dt} \simeq 0 = P - \alpha C_v C_i - \frac{C_{v,i}}{\tau_{v,i}}. \quad (5)$$

The general solution of which is given by[25]

$$C_{v,i}^{QSS} = \frac{1}{2\alpha\tau_{i,v}} \{\sqrt{1 + 4\alpha P \tau_i \tau_v} - 1\}. \quad (6)$$

The problem of void growth and swelling during steady irradiation has been previously solved using numerical integration methods.[15,17] In this section we will consider an alternate discretization technique that simplifies the calculations of point defect and void parameters without resorting to numerical integrations. The same method will also be shown to apply to pulsed irradiation. Therefore, technique-dependent differences in the swelling behavior of metals under the two modes of irradiation are eliminated.

Consider dividing the irradiation time into equal intervals, Δt, such that at the end of interval k, the time is given by

$$t^{(k)} = k\Delta t. \quad (7)$$

After k intervals, the average void radius will be given by

$$R^{(k)} = R(t^{(k)}) \quad (8)$$

and the time constants will change as the voids grow

$$\tau_{v,i}^{(k)} = \tau_{v,i}^{d}[1 + \chi^{(k)}]^{-1} \quad (9)$$

where

$$\tau_{v,i}^{d} = \frac{1}{Z_{v,i}\rho_d D_{v,i}} \quad (10)$$

and

$$\chi^{(k)} = \frac{4\pi R^{(k)} N}{\rho_d} \quad (11)$$

In the next section, we will present the analysis for steady-irradiation. The analysis depends on the dominant mode of point defect interaction.

2.2.1 Sink-Dominant Behavior If the absorption rate of point defects at sinks (such a voids, loops and dislocations) is larger than their mutual recombination rate, the solution to the equations describing point defect concentrations will simplify to:

$$C_{v,i}^{(k)} \simeq P\tau_{v,i}^{(k-1)}. \quad (12)$$

This solution is obtained from Eq. (6) if

$$4\alpha P \tau_v \tau_i \ll 1. \quad (13)$$

Let us define the net point defect flux during the interval k as

$$\phi^{(k)} = D_v C_v^{(k)} - D_i C_i^{(k)} - D_v C_v^e[e^{\xi/l_s^{(k-1)}} - 1] \quad (14)$$

where,

$$\xi = \frac{2\gamma\Omega}{R_0 k_b T_i} \quad (15)$$

and,

$$l_s^{(k-1)} = \frac{R^{(k-1)}}{R_0} \quad (16)$$

Also define

$$\phi^e = D_v C_v^e, \quad (17)$$

and

$$\phi_0^d = \frac{P\Delta Z_i}{\rho_d}, \quad \Delta Z_i = Z_i - 1. \quad (18)$$

Using these definitions, and introducing the dimensionless parameter

$$m_d = \frac{\phi^e}{\phi_0^d} \quad (19)$$

as the ratio of the emission flux of vacancies from a straight surface to the net diffusion flux, we get

$$\phi^{(k)} = \phi_0^d\{[1 + \chi^{(k-1)}]^{-2} - m_d(e^{\xi/l_s^{(k-1)}} - 1)\}. \quad (20)$$

Now, during the time interval, Δt, the void growth equation can be analytically integrated by assuming that the net vacancy flux given by Eq. (20) is approximately constant. Performing the integration and substituting for $\phi^{(k)}$, we get

$$l_s^{(k)} = l_s^{(k-1)}\left\{1 + \frac{2\Delta t\phi_0^d}{(l_s^{(k-1)}R_0)^2} \times [(1 + \chi_0 l_s^{(k-1)})^{-2} - m_d(e^{\xi/l^{(k-1)}} - 1)]\right\}^{1/2}. \quad (21)$$

This is a simple recurrence formula for $l_s^{(k)}$, and hence the steady-irradiation average void radius at any irration time.

Notice that the critical radius for void growth is obtained when $l_s^{(1)} = l_s^{(0)}$. This will lead to the

definition of the critical radius R_0^c as

$$R_0^c = \frac{\left(\frac{2\gamma\Omega}{k_B T_i}\right)}{\ln\left\{\frac{P\Delta Z_i}{\rho_d(1+\chi_0^c)^2 D_v C_v^e} + 1\right\}} \tag{22}$$

which is a simple transcendental equation in R_0^c. A similar result was obtained by Hayns.[26]

2.2.2 Point Defect Behavior Dominated by Mutual Recombination When mutual recombination dominates the behavior of point defects, simplified expressions for their quasi-steady-state concentrations can be obtained. This situation is realized if

$$4\alpha P\tau_v\tau_0 \gg 1. \tag{23}$$

In this case, Eqs. (6) approximate to

$$C_{v,i}^{(k)} \simeq \sqrt{\frac{P\tau_{v,i}^{(k)}}{\alpha\tau_{i,v}^{(k)}}}. \tag{24}$$

Substituting for the concentrations, and defining

$$\phi_0^R = \Delta Z_i\sqrt{\frac{PD_v D_i}{\alpha}} \tag{25}$$

and

$$m_R = \frac{\phi^e}{\phi_0^R} = \text{dimensionless} \tag{26}$$

we obtain the following expression for the net vacancy flux to the void

$$\phi^{(k)} = \phi_0^R\{[1+\chi_0 l_s^{(k-1)}]^{-1} - m_R[e^{\xi/l_s^{(k-1)}} - 1]\}. \tag{27}$$

Finally, the dimensionless void radius in this case will be given by

$$l_s^{(k)} = l_s^{(k-1)}\left\{1 + \frac{2\Delta t\phi_0^R}{(l_s^{(k-1)}R_0)^2} \times [(1+\chi_0 l_s^{(k-1)})^{-1} - m_R(e^{\xi/l^{(k-1)}} - 1)]\right\}^{1/2} \tag{28}$$

which is again a recurrence formula, that relates $l_s^{(k)}$ to $l_s^{(k-1)}$. The void radius at any interval, k, can be obtained by a simple progression scheme.

The critical void radius is again obtained by noting that $R^{(k)} = R_0^c$ when $l_s^{(1)} = l_s^{(0)}$. Therefore

$$R_0^c = \frac{\left(\frac{2\gamma\Omega}{K_B T_i}\right)}{\ln\left\{\frac{\Delta Z_i\sqrt{PD_v D_i/\alpha}}{(1+\chi_0^c)D_v C_v^e} + 1\right\}}. \tag{29}$$

Before we present the results of the steady-irradiation model, we will develop similar formulas for the average void radius under the irradiation conditions of ICFR's. The previous analysis will be used in comparing steady and pulsed irradiation effects on void swelling.

2.3 Void Behavior in ICFR Conditions

The behavior of voids under the irradiation conditions of ICFR's is unique in the sense that damage is produced during an extremely short period of time. For the majority of ICFR designs, the on-time is usually smaller than the interstitial mean life-time. For example, in the SOLASE conceptual reactor design,[3] the majority of the displacement damage due to neutrons occurs within 4×10^{-8} seconds. At the end of the on-time, the concentrations of both vacancies and interstitials will be approximately equal, since their diffusion to sinks is negligible within this short time. We will assume here-that the *average* damage rate over an entire cycle is P dpa/s. The amount of accumulated damage per pulse is thus

$$\varepsilon = PT_f \tag{30}$$

where T_f is the period. We define here two possible cases at the end of the on-time.

a) The on-time is smaller than the mutual recombination time $T_{on} < \tau_1$ where τ_1 is the mutual recombination time defined by Sizmann.[25]

The fractional concentrations of both vacancies and interstitials can be described by:

$$C_v(T_{on}) = C_i(T_{on}) \simeq \varepsilon \tag{31}$$

b) The on-time is longer than the mutual recombination time, but smaller than the interstitial mean lifetime ($\tau_1 < \tau_{on} < \tau_i$).

This case is achieved at low temperatures, and low to intermediate sink densities. The fractional point defect concentrations are then given by

$$C_v(T_{on}) = C_i(T_{on}) \simeq \sqrt{\frac{\varepsilon}{\alpha T_{on}}}. \tag{32}$$

Notice that the definition of τ_1 that corresponds to Sizmann's work is given by[25]

$$\tau_1 = \sqrt{\frac{T_{on}}{\alpha\varepsilon}}. \tag{33}$$

The important point here is that the concentrations of both vacancies and interstitials are equal at the end of the very short on-time.

Now, we proceed to develop the equations for point defect concentrations during any irradiation pulse. The following analysis is applicable to both cases (a) and (b). For simplicity, however, it will be restricted to case (a), while the results for (b) are readily obtained by replacing ε with $(\varepsilon/\alpha T_{on})^{1/2}$ in the final expressions. In this section, we will develop solutions to the void growth problem in the general situation where point defect behavior is governed by both diffusion to sinks and mutual recombination.

During the off-time, vacancies and interstitials will start diffusing in the medium as well as interact via mutual recombination. The source of irradiation will be absent, and their initial concentrations will be the same at the start of the first pulse. The governing equation for point defect kinetics during the first pulse is given by

$$\frac{dC_{v,i}}{dt} = -\alpha C_v C_i - C_{v,i}/\tau_{v,i}^{(1)}. \tag{34}$$

Before solving these two coupled equations, we first define an important dimensionless variable, θ, as the ratio of interstitial sink loss rate to the loss rate due to recombination at the end of the first on-time. Thus

$$\theta = (\alpha\varepsilon\tau_i^{(1)})^{-1}. \tag{35}$$

Now we will approximate the recombination loss rate in the *interstitial* equation only by assuming that $\alpha C_v C_i \simeq \alpha C_i^2$. This will effectively separate the interstitial equation from the vacancy equation, resulting in the solution

$$C_i^{(1)} = \frac{\varepsilon\theta e^{-(t-T_{on})/\tau(1)}}{1+\theta-e^{-(t-T_{on})/\tau(1)}}. \tag{36}$$

If we substitute this equation back into the vacancy equation and integrate, we get

$$C_v^{(1)} = \frac{\varepsilon\theta e^{-(t-T_{on})/\tau_v^{(1)}}}{1+\theta-e^{-(t-T_{on})/\tau_v^{(1)}}}. \tag{37}$$

Details of the manipulations leading to Eqs. (36) and (37) are given in appendix A. Since $T_f \gg \tau_i^{(1)}$, the interstitial concentration will be always close to the thermal equilibrium value by the end of the first pulse. However, the vacancy concentration will not generally decay to thermal equilibrium but will retain a certain value that is determined by the mean vacancy lifetime. Thus, the initial conditions for the interstitial and vacancy concentrations for the second pulse are:

$$C_i^{(2)}(T_{on}) = \varepsilon \tag{38}$$

and

$$C_v^{(2)}(T_{on}) = \varepsilon + \frac{\varepsilon\theta e^{-(T_f-T_{on})/\tau_v^{(1)}}}{(1+\theta)} \tag{39}$$

Now, if we use the notation

$$\eta_v^{(1)} = e^{-(T_f-T_{on})/\tau_v^{(1)}} \tag{40}$$

and

$$\eta_v^{(2)} = \frac{\eta_v^{(1)}\theta}{1+\theta}. \tag{41}$$

The initial condition (39) becomes:

$$C_v^{(2)}(T_{on}) = \varepsilon(1+\eta_v^{(2)}) \tag{42}$$

Notice that all times are now measured from the start of the second pulse. Again, if we approximate the recombination rate, $\alpha C_v C_i$, in the interstitial equation by $\alpha\{\varepsilon(1+\eta_v^{(2)})\}C_i$, we can decouple the two equations and arrive at a similar solution for the second pulse.

$$C_i^{(2)} = \frac{\varepsilon\left\{\left(\frac{Z_i+\chi^{(1)}}{Z_i+\chi_0}\right)\theta+\eta_v^{(2)}\right\}e^{-(t-T_{on})/\tau_i^{(2)}}}{1+\left\{\left(\frac{Z_i+\chi^{(1)}}{Z_i+\chi_0}\right)\theta+\eta_v^{(2)}\right\}-e^{-(t-T_{on})/\tau_i^{(2)}}} \tag{43}$$

and

$$C_v^{(2)} = \frac{(1+\eta_v^{(2)})\left\{\left(\frac{Z_i+\chi^{(1)}}{Z_i+\chi_0}\right)\theta+\eta_v^{(2)}\right\}e^{-(t-T_{on})/\tau_v^{(2)}}}{1+\left\{\left(\frac{Z_i+\chi^{(1)}}{Z_i+\chi_0}\right)\theta+\eta_v^{(2)}\right\}-e^{-(t-T_{on})/\tau_i^{(2)}}} \tag{44}$$

where

$$\tau_v^{(2)} = \left(\frac{1+\chi_0}{1+\chi^{(1)}}\right)\tau_v^{(1)} \tag{45}$$

and

$$\tau_i^{(2)} = \left\{\alpha\varepsilon\eta_v^{(2)} + \left(\frac{Z_i + \chi^{(1)}}{Z_i + \chi_0}\right)\Big/\tau_i^{(1)}\right\}^{-1}. \tag{46}$$

Following the same procedure for successive pulses, one can write the generalized equations for point defect concentrations during any pulse, k:

$$C_i^{(k)} = \frac{\left\{\left(\frac{Z_i + \chi^{(k-1)}}{Z_i + \chi_0}\right)\theta + \theta_v^{(k)}\right\}\varepsilon e^{-(t-T_{on})/\tau_i^{(k)}}}{1 + \left\{\left(\frac{Z_i + \chi^{(k-1)}}{Z_i + \chi_0}\right)\theta + \eta_v^{(k)}\right\} - e^{-(t-T_{on})/\tau_i^{(k)}}} \tag{47}$$

and

$$C_v^{(k)} = \frac{\left\{\left(\frac{Z_i + \chi^{(k-1)}}{Z_i + \chi_0}\right)\theta + \eta_v^{(k)}\right\}(1+\eta_v^{(k)})\varepsilon e^{-(t-T_{on})/\tau_v^{(k)}}}{1 + \left\{\left(\frac{Z_i + \chi^{(k-1)}}{Z_i + \chi_0}\right)\theta + \eta^{(k)}\right\} - e^{-(t-T_{on})/\tau_i^{(k)}}} \tag{48}$$

where,

$$\tau_v^{(k)} = \left(\frac{1 + \chi_0}{1 + \chi^{(k-1)}}\right)\tau_v^{(k-1)} \tag{49}$$

$$\tau_i^{(k)} = \left\{\left(\frac{Z_i + \chi^{(k-1)}}{Z_i + \chi_0}\right)\Big/\tau_i^{(k-1)} + \varepsilon\alpha\eta_v^{(k)}\right\}^{-1} \tag{50}$$

$$\eta_v^{(k)} = \frac{\left\{\left(\frac{Z_i + \chi^{(k-2)}}{Z_i + \chi_0}\right)\theta + \eta_v^{(k-1)}\right\}(1 + \eta_v^{(k-1)})\eta^{(1)}}{1 + \left\{\left(\frac{Z_i + \chi^{(k-2)}}{Z_i + \chi_0}\right)\theta + \eta_v^{(k-1)}\right\}} \tag{51}$$

Equations (47–51) are self-contained, and can be used to determine point defect concentrations during any pulse (k) and at time t measured from the start of the pulse. The validity of the solutions given by Eqs. (47) and (48) has been tested by comparing the results with more extensive calculations using numerical integration techniques. It is found that over 100 pulses the analytical solutions given by Eqs. (47) and (48) result in values that are within 2–5% of those obtained by the exact numerical integrations using the GEAR computer package.[27] It is to be noted that in our previous paper[22] simpler solutions for C_v and C_i were developed, where the microstructure was assumed to be constant during irradiation with no void sinks. The application to irradiation creep was appropriate. In the present work the equations for C_v and C_i are more general and necessary to describe the feedback effects between the void microstructure and point defect concentrations.

In order to determine the average void radius during the k'th pulse, the vacancy emission rate from the void surface will be approximated as a constant value corresponding to that at the end of the previous pulse. The net vacancy flux during the k'th pulse is then given by

$$\phi^{(k)} = \frac{Ae^{-x} - Ee^{-ax}}{B - e^{-ax}} - F \tag{52}$$

where

$$A = \left(\left\{\frac{Z_i + \chi^{(k-1)}}{Z_i + \chi_0}\right)\theta + \eta_v^{(k)}\right\}(1 + \eta_v^{(k)})\varepsilon D_v \tag{53}$$

$$B = 1 + \left\{\left(\frac{Z_i + \chi^{(k-1)}}{Z_i + \chi_0}\right)\theta + \eta_v^{(k)}\right\} \tag{54}$$

$$E = \left\{\left(\frac{Z_i + \chi^{(k-1)}}{Z_i + \chi_0}\right)\theta + \eta_v^{(k)}\right\}\varepsilon D_v \tag{55}$$

$$F = \phi^e\{e^{\xi/l_p^{(k-1)}} - 1\} \tag{56}$$

$$l_p^{(k)} = \frac{R^{(k)}}{R_0} \tag{57}$$

$$x = (t - T_{on})/\tau_v^{(k)} \tag{58}$$

and

$$a = \frac{\tau_v^{(k)}}{\tau_i^{(k)}} \gg 1 \tag{59}$$

In Eq. (52), we notice that the term e^{-ax} in the denominator plays a significant role only during the mutual recombination period that follows the end of the on-time. During this period, however, very little diffusion of point defects to voids occur and the denominator can be simply regarded as the constant B. Now, if we follow similar lines to the steady-irradiation procedure, by integrating the void growth equation within the time interval of one single pulse (T_f), we obtain for the di-

mensionless void radius $l_p^{(k)}$:

$$l_p^{(k)} \simeq l_p^{(k-1)} \times \left\{ 1 + \frac{2\phi_p}{(R_0 l_p^{k-1})^2} \left[\left\{ \frac{\left(\frac{Z_i + \chi^{(k-1)}}{Z_i + \chi_0} \right)\theta + \eta_v^{(k)}}{1 + \left(\frac{Z_i + \chi^{(k-1)}}{Z_i + \chi_0} \right)\theta + \eta_v^{(k)}} \right\} \times \left\{ \left(\frac{1 + \chi_0}{1 + \chi^{(k-1)}} \right)(1 + \eta_v^{(k)})(1 - \eta_v^{(1)}) - \frac{1}{\left(\left(\frac{Z_i + \chi^{(k-1)}}{1 + \chi_0} \right) + \frac{\eta_v^{(k)}}{\theta} \right)} \right\} - m_p [e^{\xi / l_p^{(k-1)}} - 1] \right] \right\} \tag{60}$$

where

$$\phi_p = \frac{\varepsilon}{(1 + \chi_0)\rho_d} \tag{61}$$

and

$$m_p = \frac{\phi_e (T_f - T_{on})}{\phi_p} \tag{62}$$

Equation (60) is a recurrence formula for the dimensionless void radius $l_p^{(k)}$. In the following section we will present the results of the analytical model by first comparing with previous numerical calculations for the case when the microstructure (sink densities) depend on the irradiation temperature. The comparison with the numerical solution will also establish the accuracy of the analytical procedure, and therefore will not be repeated in later sections. Finally, we will show the results when the microstructure is assumed to be temperature independent.

3 RESULTS OF THE MODEL

3.1 *Temperature Dependent Sink Densities*

The loss of point defects by intrinsic recombination introduces a source of non-linearity in the rate equations describing point defect behavior. This nonlinearity makes it difficult to develop analytical methods to the void swelling problem during steady-irradiation. Above the peak void swelling temperature, it has become usual to ignore bulk recombination and hence develop analytical solutions. Hayns[28] has recently discussed the validity of these assumptions and demonstrated that this is only true when the sink densities are temperature-independent. He also showed that the situation for temperature dependent sink densities gives almost the exact opposite result.

We have recently performed numerical calculations for a set of rate equations describing void swelling in ICFR's,[17] where realistic sink densities and material parameters were used. In this section, we compare the results of the present analytical model to previous numerical calculations. The analytical solutions for ICFR's will be further discussed in view of the Hayns[28] findings on the importance of mutual recombination.

The material parameters used in our calculations represent 316 stainless steel and are shown in Table (I). The microstructure is considered to have been already developed (past the nucleation stage) and the loop and void number densities are given by[29]

$$N_{ic} = 6.7 \times 10^{-3} \exp\{2.8(\text{eV})/k_B T\} \tag{63}$$

$$N_c = 6.5 \times 10^{8} \exp\{1.0\,(\text{eV})/k_B T\}. \tag{64}$$

These microstructure expressions were obtained by fitting the experimental data of electron irradiated stainless steel, where collision cascades are absent.[29] The results of this section apply only to the growth phase of void swelling, and the calculations start with a preconditioned microstructure. The results of the growth calculations are therefore not necessarily dependent upon the initial microstructure. For consistent loop and void

TABLE I

Material parameters for stainless steel (Ref. 29)

Parameter	Units	Value
Z_i	—	1.08
Z_v	—	1.00
D_i^v	m^2/s	10^{-7}
D_v	m^2/s	5×10^{-5}
E_i^m	J	3.2×10^{-20}
E_v^m	J	2.1×10^{-19}
α/D_i	m^{-2}	10^{20}
Ω	m^3	8×10^{-30}
γ	J/m^2	2
E_v^f	J	2.56×10^{-19}
E_i^f	J	6.41×10^{-19}

number densities, however, we use electron irradiation results in this section and neutron irradiation data in the next section.

Two main factors contribute to the difference in the behavior of voids during steady and pulsed irradiation conditions. The high damage rates in pulsed irradiation increase the fraction of recombining point defects. The second process is an increased rate of vacancy emission from the void surface because of its slower growth due to the shrinkage transient associated with the interstitial absorption. In order to understand the importance of these processes, we compare the results of the present analytical model to the more general numerical calculations of Ref. (17). In Figure (1), the parameter θ is plotted as a function of the pulsing frequency, ω. The microstructure described by Eqs. (63) and (64) was used in calculating θ at various temperatures. The importance of point defect mutual recombination is shown to increase with increasing temperature for any given number of pulses. This point was clearly demonstrated by Hayns[28] in his steady-irradiation calculations. An interesting feature of Figure (1) is the greater role of recombination for the low pulsing frequencies. A low pulsing frequency with the same average damage rate implies that the damage per pulse is high, and consequently, so is the amount of recombination.

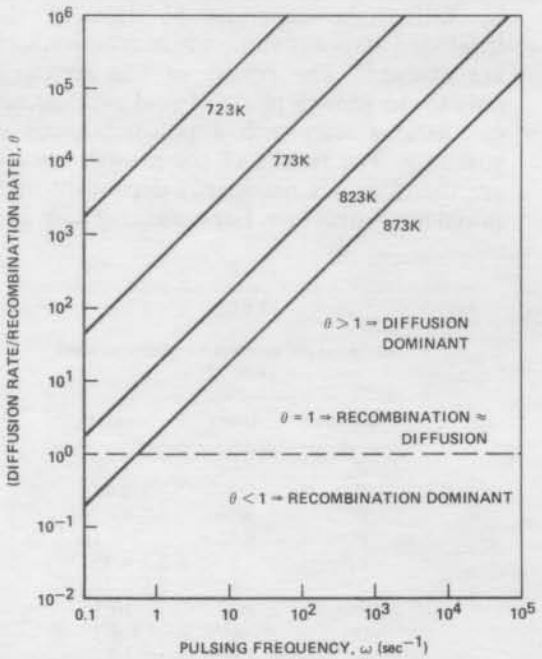

FIGURE 1 The ratio of the interstitial diffusion rate to recombination rate (θ) plotted as a function of the pulsing frequency, ω for the temperature dependent microstructure.

Figure 2 shows a comparison between the previous numerical calculations[17] and the present analytical method. The figure shows the change in the void radius as a function of the frequency for a given amount of total displacement damage (10^{-5} dpa). The agreement between the analytical and numerical calculations is fairly good. It is also shown that for the high temperature 823 K, the combined effects of mutual recombination and interpulse annealing result in significantly slower void growth rates at lower pulsing frequencies.

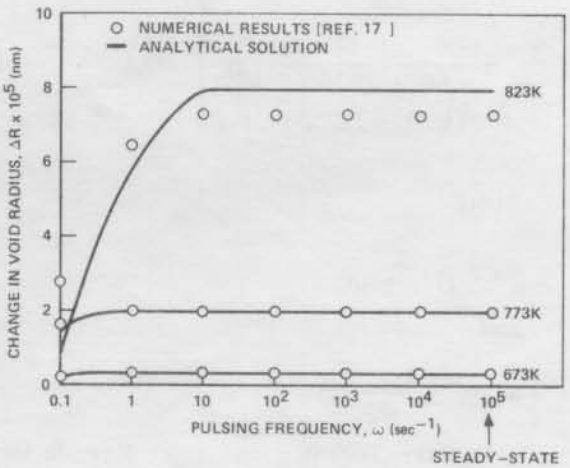

FIGURE 2 A comparison between the numerical and analytical results for the change in void radius as a function of the pulsing frequency, ω, $Z_i = 1.08$, $T_{an} = 10^{-7}$ sec, $R_c(0) = 10$ nm, and average dose rate $= 10^{-6}$ dpa/s.

Figure 3 shows a summary of the results of void growth as a function of irradiation temperature at various pulsing frequencies. The microstructure described by Eqs. (63) and (64) was again used, with an initial void radius of 10 nm. Steady-irradiation void growth is small at low temperatures due to the high sink densities. At high temperatures, voids tend to evaporate by vacancy emission resulting in the elimination of void swelling for temperatures that are higher than ~890 K. Intense radiation pulsing changes this void growth behavior. At the low temperature end, the pulsing effects are shown not to be very significant. Intrinsic recombination and interpulse annealing both play a minor role at low temperatures, and the differences between steady and pulsed irradiation results are small. As the temperature is increased, point defect recombination and void

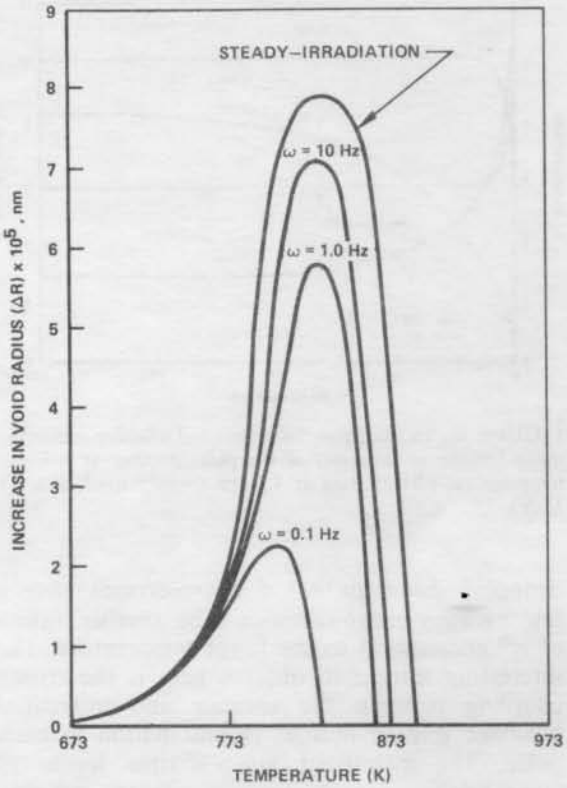

FIGURE 3 The increase in the average void radius as a function of irradiation temperature for various pulsing frequencies. $R_c(0) = 10$ nm, $T_{on} = 10^{-7}$ sec, $Z_i = 1.08$, and average dose rate $= 10^{-6}$ dpa/s.

annealing become important producing slower void growth. The peak void growth is shown to be lowered for the smaller frequencies, and the peak swelling temperature is slightly smaller. The void growth cut-off temperature is also lowered due to pulsing. It decreases by as much as 60 K for a pulsing frequency of 0.1 Hz.

3.2 Temperature Independent Sink Densities

The number densities of voids and interstitial loops is experimentally established to decrease as the irradiation temperature increases.[18] This is the case if one starts with a fresh metal that has not been irradiated before. The temperature dependence of the microstructure complicates the understanding of the way point defects are partitioned between various sinks versus mutual recombination. Another method to study the response of materials to irradiation is to pre-condition the irradiated material with a desired microstructure. To illustrate various aspects of pulsed irradiation effects, we choose here to use a temperature independent microstructure that corresponds to the EBR-II irradiation conditions at 823 K. This microstructure was chosen at a neutron fluence of 10^{26} n/m^2 of energy >0.1 MeV (~ 4.7 dpa). At this fluence, the void density is $\sim 1.3 \times 10^{19}$ voids/m^3, the average void radius is ~ 11 nm and the dislocation density is $\sim 2 \times 10^{13}$ m^{-2}.[24]

Since the microstructure was assumed to be temperature independent, the parameter θ will also be insensitive to temperature variations. Notice that θ depends primarily on the behavior of interstitials, which is not very sensitive to temperature. In Figure 4, the parameter θ is shown as a function of the pulsing frequency. The intrinsic recombination starts to become important for frequencies lower than ~ 100 Hz and dominant for frequencies lower than ~ 5 Hz.

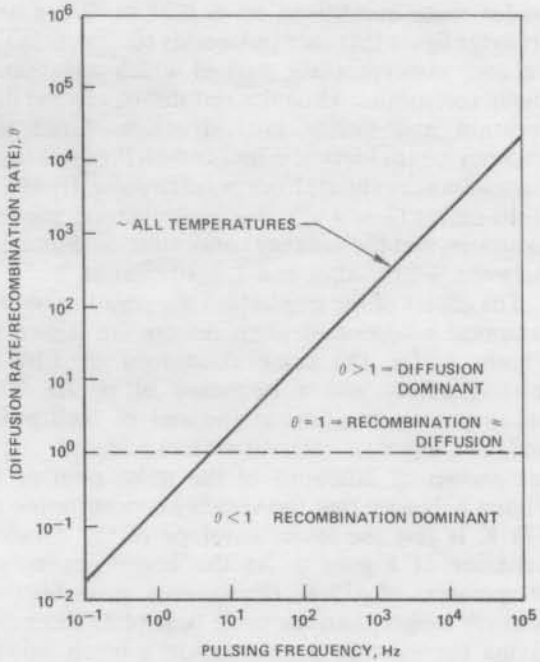

FIGURE 4 The ratio of the interstitial diffusion rate to recombination rate as a function of the frequency for a temperature independent microstructure that corresponds to EBR-II at 4.7 dpa and 823 K.

The vacancy concentration at 773 K for a pulsing frequency of 10 Hz and the initial conditions of the chosen EBR-II microstructure, is shown as a function of the irradiation time in Figure 5. The vacancy mean-lifetime is 0.23 seconds

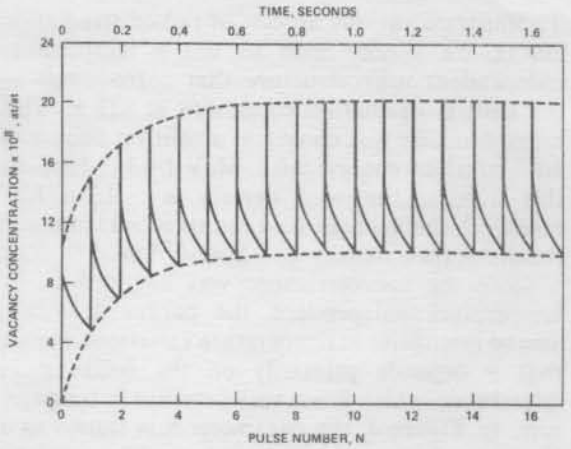

FIGURE 5 The detailed behavior of the vacancy concentration as a function of time at a temperature of 773 K and $\omega = 10$ Hz for the microstructure of Figure 4.

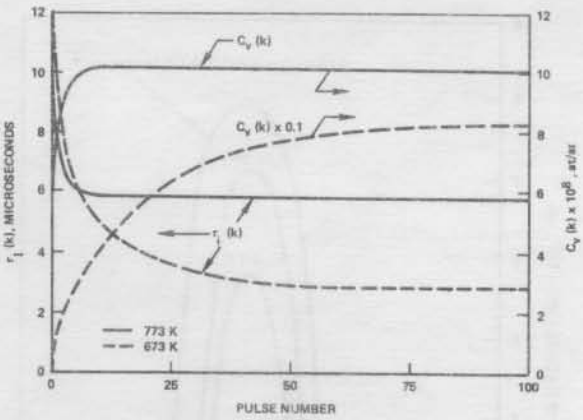

FIGURE 6 Vacancy concentrations and effective interstitial mean lifetime as functions of the pulse number at different temperature. EBR-II data at 4.7 dpa ($\sim 10^{26}$ n/m^2, $E > 0.1$ MeV).

under these conditions ($\tau_v^0 \simeq 0.23$ s). We notice from the figure that each pulse adds 10^{-7} at/at to the vacancy concentration, part of which instantaneously recombine, while the rest diffuses to the dislocation and cavity microstructure. Since the vacancy means lifetime is longer than the cycle time, vacancies accumulate from pulse to pulse. By about 9–10 pulses ($3 \sim 4\ \tau_v^0$), this accumulation process saturates, and the vacancy concentration fluctuates between $\sim 10^{-7}$ at/at and 2×10^{-7} at/at.

The effects of the irradiation temperature on the temporal behavior of point defects are shown in Figure 6, for the same conditions of EBR-II microstructure and a frequency of 10 Hz. The vacancy concentration at the end of each pulse and the effective interstitial mean-lifetime ($\tau_i^{(k)}$) are shown as functions of the pulse number in Figure 6. Notice that the vacancy concentration at 773 K is just the lower envelope of the detailed behavior of Figure 5. At the lower irradiation temperature of 673 K, the vacancy mean-lifetime is much longer than the cycle time (4.23 seconds), giving the vacancy concentration a much slower rate of increase. After about 100–150 pulses, the vacancy concentration saturates at a value that is almost an order of magnitude higher than at 773 K. The concentration fluctuates between $\sim 8 \times 10^{-7}$ at/at and 9×10^{-7} at/at. The behavior of interstitials can be studied by examining the effective interstitial mean-lifetime. The interstitial mean lifetime is not very sensitive to the irradiation temperature, starting at values of 8–12 microseconds at the beginning of irradiation and dropping down to $\sim$3–6 microseconds after a few vacancy mean-lifetimes. The smaller values of $\tau_i^{(k)}$ correspond to the lower temperature. The interesting feature to observe here is the strong coupling between the vacancy and interstitial behavior due to mutual recombination in each pulse. The interstitial mean-lifetime levels off (except for a slow decrease due to the growing microstructure) at about the same time vacancies achieve a repeatable fluctuating behavior.

Figure 7 shows the change in the average void radius of the same EBR-II microstructure at 673 K and 773 K. The average void responds to the temporal fluctuations in point defect concentrations by a shrinkage transient followed by a growth rate that is always slower than the corresponding steady-irradiation. The initial void shrinkage is attributed to the rapid arrival of interstitial atoms to the void surface in consecutive pulses. Once the point defect concentrations reach a state of repeatable profiles from pulse to pulse (in ~ 2–$3\ \tau_v$), there will always be an excess of vacancies reaching the void with each pulse. At this time the shrinkage transient is reversed, and a slower increase in the radius than the corresponding steady-irradiation commences (after ~ 10 pulses at 773 K and 150 pulses at 673 K). The slower increase in the average radius of the void under pulsed irradiation is partly due to the enhanced recombination of point defects, and partly because of the higher vacancy emission rate of the smaller size void. Finally, Figure 8 shows the change in the void radius as a function of irradiation time for various

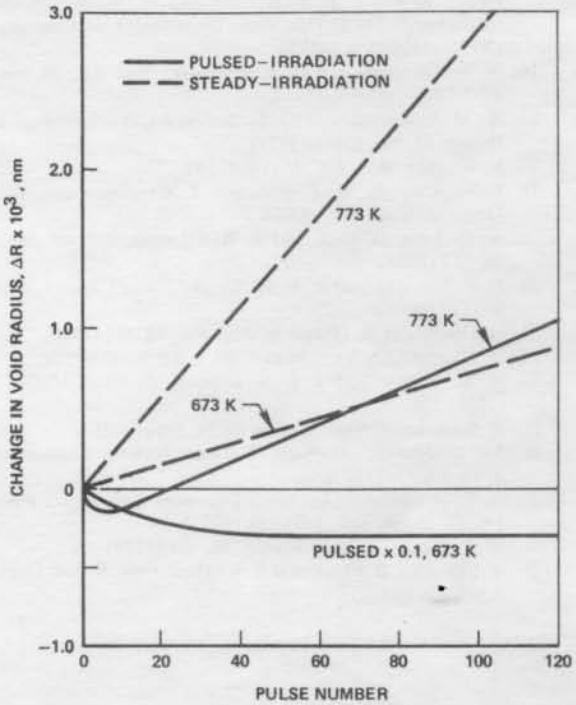

FIGURE 7 A comparison between steady and pulsed irradiation results for the EBR-II data and $R_c(0) = 11$ nm.

pulsing frequencies at the same temperature of 823 K and the EBR-II microstructure. The steady-irradiation void growth rate is seen to be the fastest. It is also indicated that the lower the frequency, the slower the void growth rate.

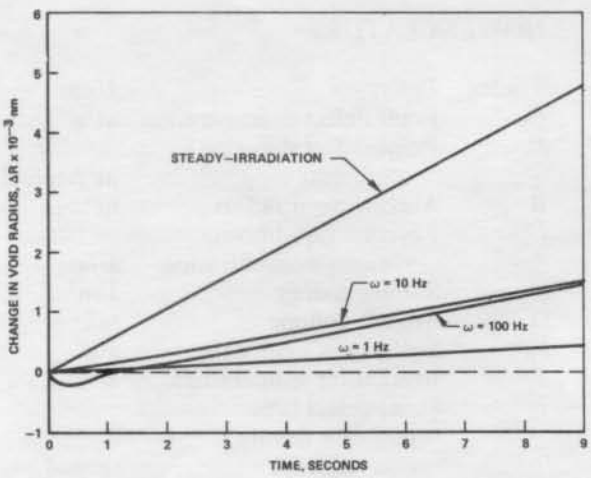

FIGURE 8 The change in void radius as a function of irradiation time for steady and pulsed irradiation at various frequencies. Irradiation temperature = 823 K.

4 SUMMARY AND CONCLUSIONS

In this paper, we have developed an analytical model to study the problem of void growth in metals subjected to intense radiation pulsing. The analytical formulas developed for the dynamic behavior of point defects and voids agree to within a few percent with the more extensive numerical integrations that have been previously reported.

The swelling of metals due to void growth without collision cascades under intense radiation pulsing was concluded to be generally smaller than the corresponding steady irradiation. The magnitude of point defect mutual recombination can be accurately determined by the present analytical model. As a consequence of the increased rate of recombination due to the high damage rates in pulsed systems, the void growth rate is generally lower. Void shrinkage transients result from the rapid diffusion of interstitials. Vacancy emission is thus enhanced, and void growth will become even slower at temperatures above approximately half of the melting point.

When the microstructure is temperature dependent, void growth is particularly retarded at high temperatures. Recombination and interpulse annealing become dominant at temperatures above the peak swelling temperature. Pulsing frequency was shown to have a profound effect on both the magnitude of the maximum swelling rate and on the swelling cut-off-temperature. Low pulsing frequencies reduce the maximum void growth rate as well as the swelling cut-off temperature.

ACKNOWLEDGEMENTS

We are grateful for the support provided by the National Science Foundation through Grant Nos. ENG78–05413 and ENG78–05554. Also, the partial support of the University of Wisconsin through sub-contract number D800131 is gratefully acknowledged.

REFERENCES

1. B. Badger, *et al.*, UWMAK-III, A non-circular tokamak power reactor design, *Electric Power Research Institute Report* ER-368, EPRI, July (1976).
2. B. Badger, *et al.*, NUWMAK, A tokamak reactor design study, *University of Wisconsin Fusion Design Report*, UWFDM-330, March (1979).
3. R. W. Conn, *et al.*, (Solace: A Laser Fusion Reactor Study), *University of Wisconsin Fusion Design Report*, UWFDM-220, December (1977).

4. T. O. Hunter and G. L. Kulcinski, *J. Nucl. Mater.*, **76**, 383 (1978).
5. S. A. Metz and F. A. Smidt, Jr., *Appl Phys. Lett.*, **19**, 207 (1971).
6. F. A. Smidt, Jr., and S. A. Metz, *Proc. of Conf. on Radiation Induced Voids in Metals*, Albany, New York, 613, June (1971).
7. H. Kressel and N. Brown, *J. Appl. Phys.*, **38**, 1613 (1967).
8. J. A. Sprague and F. A. Smidt, Jr., *NRL Memorandum Report* 2629 (1973).
9. A. Taylor, *et al.*, Argonne National Laboratory Report, ANL/CTR/TM-39 (1975).
10. R. A. Powell and G. R. Odette, *J. Nucl. Mat.*, **85/86**, 695 (1979).
11. D. Kaletta, *J. Nucl. Mat.*, **85/86**, 775 (1979).
12. N. M. Ghoniem and G. Kulcinski, *American Nuclear Society Transactions*, **30**, 149 (1978).
13. G. R. Odette and R. Myers, *Hanford Laboratory CTR Quarterly Prog. Report*, HEDL TME/7590, April–June (1975) 2.
14. Y. H. Choi, A. L. Bement, and K. C. Russell, *Proc. of Conf. on Radiation Effects and Tritium Technology for Fusion Reactors*, J. S. Watson and F. W. Wiffen, eds., Gatlinburg, TN (1975), U.S. Department of Commerce, CONF-750989, p. II-1.
15. J. O. Schiffgens, J. N. Graves and D. G. Doran, *Proc. of Conf. on Radiation Effects and Tritium Technology for Fusion Reactors*, J. S. Watson and F. W. Wiffen, eds., Gatlinburg, TN (1975), U.S. Department of Commerce, CONF-750989, p. I-532.
16. N. M. Ghoneim and G. L. Kulcinski, *Rad. Eff.*, **39**, No. 1, 47 (1978).
17. N. M. Ghoniem and G. L. Kulcinski, *Nuclear Eng. and Design*, **52**, No. 1, 111 (1979).
18. K. Krishan, *Rad. Eff.*, **45** (1980) 169.
19. L. N. Kmetyk, W. F. Sommer, J. Weertman and W. V. Green, *J. Nucl. Mat.*, **85/86**, 553 (1979).
20. N. Q. Lam, G. Leaf, and R. A. Johnson, *J. Nucl. Mater.*, **74**, 277 (1978).
21. E. P. Simonen and P. L. Hendrick, *J. Nucl. Mater.*, **85/86**, 873 (1979).
22. H. Gurol and N. Ghoniem, *Rad. Eff.*, **52**, 103 (1980).
23. N. Ghoniem, *J. Nucl. Mater.*, **89**, 2 and 3 (1980) 359.
24. H. R. Brager and J. L. Straalsund, *J. Nucl. Mater.*, **46** (1973) 134.
25. R. Sizmann, *J. Nucl. Mater.*, **69/70**, 386 (1978).
26. M. R. Hayns, *American Nuclear Society Transactions*, ANS, **27**, 328 (1977).
27. A. E. Hindmarsh, *Lawrence Livermore Laboratory Report* UCID-30059, Rev. 1, March (1975).
28. M. R. Hayns, *J. Nucl. Mater.*, **79**, 323 (1979).
29. R. Bullough, B. Eyres, and R. Krishan, *Proc. R. Soc. London*, A346, 81 (1975).

Appendix A

POINT DEFECT CONCENTRATIONS IN ICFR's

To determine the concentrations of point defects during the off-time starting from Eq. (34) and the initial conditions given by Eq. (31), we first solve the interstitial equation by setting $C_v \simeq C_i$ in the recombination rate:

$$\frac{dC_i}{dt} \approx -\alpha C_i^2 - C_i/\tau_i^{(1)}. \tag{A.1}$$

Upon integration, the solution of (A.1) is given by:

$$\log_e\left\{\frac{C_i/\varepsilon}{[C_i + (\alpha\tau_i^{(1)})^{-1}]/[\varepsilon + (\alpha\tau_i^{(1)})^{-1}]}\right\} = -t/\tau_i^{(1)}. \tag{A.2}$$

Upon rearranging Eq. (A.2), we can easily obtain Eq. (36). Now, substituting Eq. (36) back into Eq. (34), we get

$$\frac{dC_v}{dt} = -\frac{\alpha\varepsilon\theta C_v}{[(1+\theta)e^{(t-T_{on})/\tau_i^{(1)}} - 1]} \tag{A.3}$$

which can be integrated by separation of variables to obtain Eq. (37).

NOMENCLATURE

Symbol	*Definition*	*Units*
$C_{i,v}$	Point defect concentration	at/at
$D_{v,i}$	Point defect diffusion coefficient	m^2/second
R	Average void radius	m
C_v^e	Thermal Equilibrium vacancy concentration	at/at
γ	Surface energy	J/m^2
Ω	Atomic volume	m^3
k_B	Boltzmann's constant	J/K
T_i	Irradiation temperature	K
$\tau_{v,i}^{(k)}$	Point defect time constant during interval k	second
$Z_{v,i}$	Dislocation bias to point defects	—

Symbol	*Definition*	*Units*
ρ_d	Dislocation density	m^{-2}
N	Cavity number density	m^{-3}
α	Point defect recombination coefficient	$second^{-1}$
P	Average displacement rate	at/at/second
Δt	Time interval	second
R_0	Initial cavity radius	m
R_0^c	Critical cavity radius	m
ε	Accumulated damage per pulse	at/at
T_{on}	On-time	second
T_f	Cycle time	second
θ	Ratio of interstitial sink diffusion to recombination rate at the end of the first on-time	